Formation of Both Primary and Secondary *N*-Alkylhemins during Hemin-Catalyzed Epoxidation of Terminal Alkenes

Zong-Qiang Tian,*,† Joseph L. Richards,‡ and Teddy G. Traylor§

Contribution from the Department of Chemistry, University of California, San Diego, 9500 Gilman Drive, La Jolla, California 92037-0506

Received August 2, 1993. Revised Manuscript Received April 29, 1994⊗

Abstract: The *N*-alkylhemin formation during iron(III) porphyrin-catalyzed epoxidation of alkenes is studied in a homogeneous system using pentafluoroiodosobenzene (PFIB) as the oxidant. The system is a model for the enzyme cytochrome P-450. A second *N*-alkyl species other than the well-documented primary *N*-alkylhemin is observed during the oxidation of terminal alkenes. It is unstable and decomposes under the reaction conditions. It is also a catalyst for alkene epoxidation by PFIB. Its characteristics are consistent with a secondary *N*-alkylhemin. The kinetics were partially resolved, and rate constants were estimated for the formation of both *N*-alkylhemins, for the decomposition of the secondary *N*-alkylhemin, and for the epoxidation by the hemin and the *N*-alkylhemins. The partition ratios were measured by a kinetic method, which provides better insight for the mechanisms of both *N*-alkylation and epoxidation than the measurements by product analysis using heterogeneous systems. We suggest that alkenes reversibly inhibit cytochrome P-450 through the formation of the unstable *N*-alkylporphyrin species.

Suicide inactivation of cytochromes P-450 during oxidation of alkenes and alkynes catalyzed by these enzymes involves the alkylation of the porphyrins at a pyrrolic nitrogen.[1] Most of the substrates found to cause suicide inactivation are terminal alkenes, and the isolated porphyrin product contains an *N*-substituent attached at the primary carbon (Figure 1).[2] Synthetic models of cytochromes P-450 also form *N*-alkylhemins with both terminal and nonterminal alkenes.[3−6] Unlike the enzymes, however, the synthetic *N*-alkylhemins were found to catalyze the epoxidation of alkenes (Scheme 1).[5]

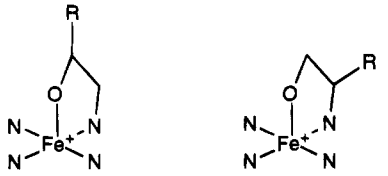

The structure proposed for *N*-alkylhemins contains a five-membered metallocycle as shown in Figure 2A. The existence of such an iron porphyrin structure has been established by X-ray crystallography (Figure 2B).[7] With terminal alkenes, there exist two possible regioisomers for the *N*-alkylhemins. Either the primary or the secondary carbon may be attached to the pyrrolic nitrogen. These two possible isomers are designated as primary *N*-alkylhemins and secondary *N*-alkylhemins, respectively. Although the *N*-alkylhemins isolated and characterized are mostly primary *N*-alkylhemins,[4,8] secondary *N*-alkylhemins have

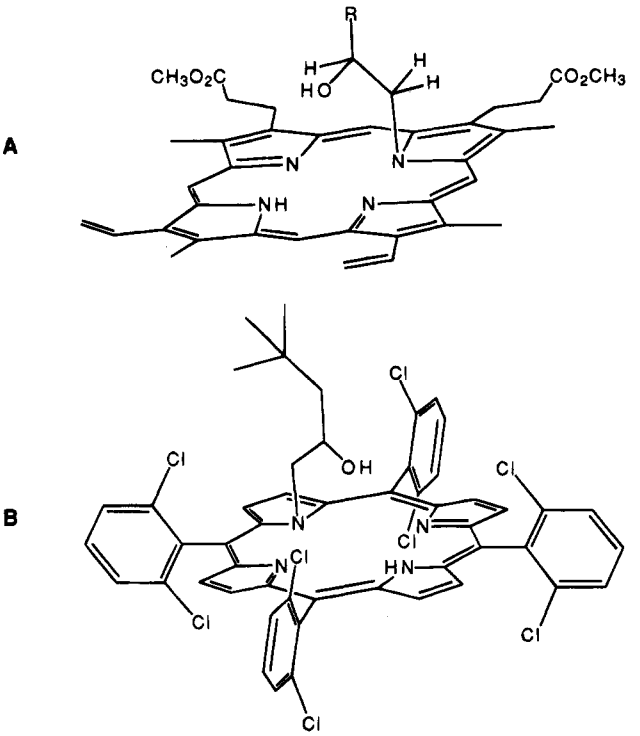

Figure 1. Structures for primary *N*-alkylporphyrins: (A) *N*-alkylporphyrin isolated from phenobarbital-induced rat cytochrome P-450 inactivated by terminal alkenes (ref 2); (B) *N*-alkylporphyrin product from TDCPPFeCl-catalyzed oxidation of 4,4-dimethyl-1-pentene by PFIB (ref 4a).

* Please address reprint requests to C. L. Perrin, Department of Chemistry, University of California, San Diego, 9500 Gilman Drive, La Jolla, CA 92037-0506.

† Current address: Department of Chemistry, University of California, Berkeley, CA 94720-1460.

‡ Current address: Department of Chemistry, Grand Valley State University, 1 Campus Drive, Allendale, MI 49401-9403.

§ Deceased, June 14, 1993.

⊗ Abstract published in *Advance ACS Abstracts,* December 1, 1994.

(1) (a) Ortiz de Montellano, P. R.; Correia, M. A. *Annu. Rev. Pharmacol. Toxicol.* **1983**, *23*, 481−503. (b) Holley, A. E.; Frater, Y.; Gibbs, A. H.; De Matteis, F.; Lamb, J. H.; Farmer, P. B.; Naylor, S. *Biochem. J.* **1991**, *274*, 843−848.

(2) Kunze, K. L.; Mangold, B. L. K.; Wheeler, C.; Beilan, H. S.; Ortiz de Montellano, P. R. *J. Biol. Chem.* **1983**, *258*, 4202−4207.

(3) (a) Mansuy, D.; Devocelle, L.; Artaud, I.; Battioni, J.-P. *New J. Chem.* **1985**, *9*, 711−716. (b) Artaud, I.; Devocelle, L.; Battioni, J.-P.; Girault, J. P.; Mansuy, D. *J. Am. Chem. Soc.* **1987**, *109*, 3782−3783. (c) Artaud, I.; Gregoire, N.; Mansuy, D. *New J. Chem.* **1989**, *13*, 581−586.

(4) (a) Mashiko, T.; Dolphin, D.; Nakano, T.; Traylor, T. G. *J. Am. Chem. Soc.* **1985**, *107*, 3735−3736. (b) Nakano, T.; Traylor, T. G.; Dolphin, D. *Can. J. Chem.* **1990**, *68*, 1504−1506.

(5) Traylor, T. G.; Nakano, T.; Miksztal, A. R.; Dunlap, B. E. *J. Am. Chem. Soc.* **1987**, *109*, 3625−3632.

(6) Collman, J. P.; Hampton, P. D.; Brauman, J. I. *J. Am. Chem. Soc.* **1990**, *112*, 2977−2986.

(7) Battioni, J.-P.; Artaud, I.; Dupré, D.; Leduc, P.; Akhrem, I.; Mansuy, D.; Fischer, J.; Weiss, R.; Morgenstern-Badarau, I. *J. Am. Chem. Soc.* **1986**, *108*, 5598−5607.

0002-7863/95/1517-0021$09.00/0

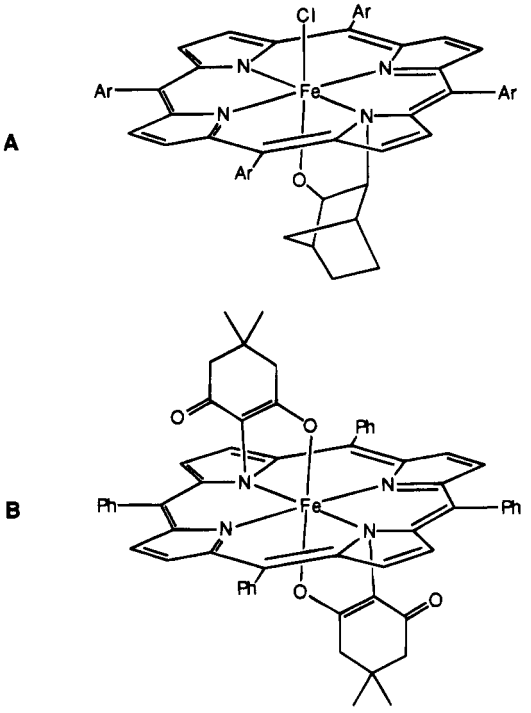

Figure 2. Structures for secondary *N*-alkylhemins: (A) structure proposed for the *N*-alkylhemin formed during iron(III) tetraarylporphyrin-catalyzed oxidation of norbornene using PFIB as the oxidant (ref 5); (B) *N,N*-bis-alkylated Fe(II)TPP complex from reaction of Fe(II)TPP with an iodonium ylide. The structure was established by X-ray crystallography (ref 7).

Scheme 1. Proposed Pathway for Hemin-Catalyzed Epoxidation of Alkenes Showing the Accompanying Catalysis by *N*-Alkylhemin

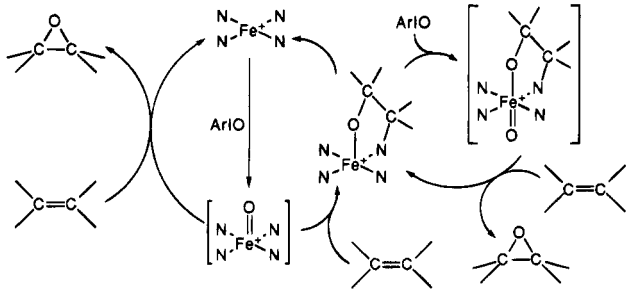

been observed as transient species during oxidation of nonterminal alkenes,[3c,5,9,10] e.g., norbornene and *trans*-2-hexene. Some secondary *N*-alkylhemins are stable enough at low temperatures to allow isolation and subsequent characterization of the demetalated *N*-alkylporphyrins.[3c,10]

During hemin-catalyzed epoxidation of terminal alkenes, an intermediate is observed having a visible spectrum similar to that of a primary *N*-alkylhemin (λ_{max} 435 nm), but it is much less stable. The most reasonable assignment for this intermediate is the secondary *N*-alkylhemin. In this paper we report our studies on the formation of both primary and secondary *N*-alkylhemins by terminal alkenes.

Experimental Section

Materials. Allyltrimethylsilane (Aldrich, 98%) was either distilled under argon or passed through a neutral alumina column before use. Methanol (Fisher, spectroanalytical grade), 2,2,2-trifluoroethanol (Aldrich, 99.5+%), 4,4-dimethyl-1-pentene (Pfaltz & Bauer, 99%), styrene (Pfaltz & Bauer, 99%), vinylcyclohexane (Aldrich, 99+%), allyl cyanide (Aldrich, 98%), *trans*-cyclohexane-1,2-diol (Aldrich, 98%), and pentafluoroiodobenzene (Aldrich, 99%) were used as received. Norbornene (Aldrich, 99%) and 2,5-norbornadiene (Aldrich, 99%) were distilled under argon. Allyl chloride (Aldrich, 98%) was purified by passage through a neutral alumina column before use. Dichloromethane (Fisher reagent grade) was distilled over CaH_2 under nitrogen before use. Water was doubly deionized.

[5,10,15,20-Tetrakis(2,6-dichlorophenyl)porphinato]iron(III) chloride (TDCPPFeCl) and [5,10,15,20-tetra-*o*-tolylporphinato]iron(III) chloride (TTPFeCl) were prepared and purified by literature methods.[10-13]

Pentafluoroiodosobenzene (PFIB) was prepared following the literature procedures.[6,14-16] The purity was at least 97% by iodometric titrations.[17] ^{19}F NMR (CD_3OD): δ 5.44 (m, 2 F, *m*-F's), 15.31 (t, J = 20 Hz, 1 F, *p*-F's), 40.14 (d, J = 20 Hz, 2 F, *o*-F's).

Instruments. UV−vis spectra and slow kinetic data were recorded on Kontron Uvikon 810 spectrophotometers interfaced with a Celerity mainframe computer or a Zenith microcomputer. Rapid repetive scan spectroscopy was performed with either a Hewlett-Packard 8450A spectrophotometer or an optical multichannel analyzer consisting of a Princeton Applied Research 1215 OMA console with 1218 controller and 1229 spectrograph. The light source for the OMA was a 100-W tungsten lamp, lens collimated and filtered through 2 cm of 250 g/L $CuSO_4 \cdot 5H_2O$ solution and then through 2 cm of 25 g/L $CoSO_4 \cdot 7H_2O$ solution. Fast kinetic data were obtained on a Hi-Tech Scientific stopped-flow instrument consisting of SFL-43, SF-3L, and SU-40A units with the multimix unit disconnected, and the voltage output was collected on a Zenith Z-100 PC equipped with a Metrobyte Dash-8 A/D converter. A Hamamatsu R374 photomultiplier was used in substitution of the Hi-Tech PM-60 photomultiplier. A Hi-Tech Model SFA-11 stopped-flow unit was operated in the HP spectrophotometer, the Kontron spectrophotometer, or the OMA units. Both of the stopped-flow instruments had a dual path of 2 mm or 1 cm. All the kinetic measurements were performed at 25 °C.

Gas chromatography was performed on a Varian 3700 gas−liquid chromatograph, operating in the flame ionization mode, fitted with a 1.8 m × 3.2 mm i.d. (6 ft × 1/8 in.) column of 10% Carbowax 20M on 100/120 Supelcoport.

NMR spectra were obtained on a Varian Unity 500 FT-NMR spectrometer operating at 500 MHz (470 MHz for ^{19}F). ^{19}F chemical shifts are relative to internal hexafluorobenzene as 0 ppm.

Rapid Spectroscopy. The rapid spectral change in the visible region was observed using the OMA and the SFA-11 stopped-flow instruments. A solution of 1 M alkene and 2 × 10^{-5} M TDCPPFeCl in 80:18:2 (v/v) $CH_2Cl_2/CF_3CH_2OH/H_2O$ was placed in one syringe, and a solution of 0.017 M PFIB in the same solvent was placed in the other. The solutions were mixed in equal volumes, and data collection was started after mixing was completed. The syringes were driven by hand. The formation of *N*-alkylhemins was also studied at lower concentrations of PFIB (e.g. 5 × 10^{-4} M) and TDCPPFeCl (e.g. 1 × 10^{-6} M) on the HP spectrophotometer. A solution containing allyltrimethylsilane (1 M) and TDCPPFeCl in 80:18:2 (v/v) $CH_2Cl_2/CF_3CH_2OH/H_2O$ and a solution of PFIB in the same solvent were mixed in equal volumes in a sealed 1-cm cuvette by shaking, and sequential UV−vis spectra were recorded starting 5−6 s after mixing.

Hemin-Catalyzed Epoxidation Quenched by *trans*-Cyclohexane-1,2-diol. A solution of allyltrimethylsilane and TDCPPFeCl in 80:18:2 (v/v) $CH_2Cl_2/CF_3CH_2OH/H_2O$ was placed in a sealed vial fitted

(8) Collman, J. P.; Hampton, P. D.; Brauman, J. I. *J. Am. Chem. Soc.* **1986**, *108*, 7861−7862.
(9) Traylor, T. G.; Miksztal, A. R. *J. Am. Chem. Soc.* **1987**, *109*, 2770−2774.
(10) Dunlap, B. E. Ph.D. Dissertation, University of California at San Diego, 1988.
(11) Kobayashi, H.; Higuchi, T.; Kaizu, Y.; Osada, H.; Aoki, M. *Bull. Chem. Soc. Jpn.* **1975**, *48*, 3137−3141.
(12) Kim, J. B.; Leonard, J. J.; Longo, F. R. *J. Am. Chem. Soc.* **1972**, *94*, 3986−3992.
(13) Traylor, P. S.; Dolphin, D.; Traylor, T. G. *J. Chem. Soc., Chem. Commun.* **1984**, 279−280.
(14) Schmeisser, M.; Dahmen, K.; Sartori, P. *Chem. Ber.* **1967**, *100*, 1663−1669.
(15) Saltzman, H.; Sharefkin, J. G. *Organic Syntheses*; Wiley: New York, 1973; Collect. Vol. V, pp 658−659.
(16) Collman, J. P. *Chem. Eng. News* **1985**, *63* (11), 2.
(17) Vogel, A. I. *Quantitative Inorganic Analysis*, 3rd ed.; Wiley: New York, 1961; p 34.

with two syringes through a poly(tetrafluoroethene) septum. One of the syringes contained a solution of PFIB, and the other contained 50 μL of 1 M *trans*-cyclohexane-1,2-diol (CHD) in the same solvent. The PFIB solution was rapidly injected into the vial to obtain a 500-μL solution containing 0.5 M allyltrimethylsilane, 1×10^{-6} M TDCPPFeCl, and 5×10^{-4} M PFIB. After the mixture was stirred for a given time, the reaction was quenched by injecting the CHD solution into the vial. A final UV−vis spectrum was recorded after 20−30 min.

Kinetics of *N*-Alkylhemin Formation. The formation of *N*-alkylhemins by norbornene, norbornadiene, vinylcyclohexane, styrene, and 4,4-dimethyl-1-pentene in 89:10:1 (v/v) $CH_2Cl_2/CF_3CH_2OH/H_2O$ and allyltrimethylsilane in both 89:10:1 and 80:18:2 (v/v) $CH_2Cl_2/CF_3CH_2OH/H_2O$ solvents was studied by stopped-flow spectrophotometry. In one of the two equal volume syringes was placed a solution of a substrate alkene (0.5−1 M) with TDCPPFeCl ($(1-2) \times 10^{-5}$ M) in $CH_2Cl_2/CF_3CH_2OH/H_2O$ mixed solvent. The second syringe contained a solution of PFIB (2−8 mM) in the same solvent. The syringes of the SFL-43 unit were driven by 550-kPA (80-psi) air pressure, and the typical mixing time was within 20 ms. At the termination of mixing, the voltage output from the photomultiplier at one wavelength (typically at 410 or 435 nm) was recorded vs time, which was then converted to absorbance vs time. The kinetics of epoxidation of and slow *N*-alkylation by 4,4-dimethyl-1-pentene and allyltrimethylsilane were studied by observing the absorbance change at wavelengths around 250−280 nm, and 410 or 435 nm, respectively, on the Kontron spectrophotometer. Stock solutions were made for 4,4-dimethyl-1-pentene (1 M), allyltrimethylsilane (1.6 M), TDCPPFeCl (1×10^{-5} M), and PFIB (2×10^{-3} M) in 89:10:1 (v/v) $CH_2Cl_2/CF_3CH_2OH/H_2O$. An alkene solution and the TDCPPFeCl solution were mixed with a calculated volume of the solvent, and the PFIB solution was added last, to achieve various initial concentrations of TDCPPFeCl and PFIB. The absorbance change at a wavelength was recorded vs time as soon as the cuvette was in place (3−7 s after addition of PFIB). A final UV−vis spectrum was recorded for each kinetic-run after 20−30 min. Kinetic data were processed either on an Apple Macintosh II microcomputer using Microsoft Excel and WaveMetrics Igor programs or on a Celerity mainframe computer.

Product Analysis of *N*-Alkylhemin Decomposition. To a solution of TTPFeCl (0.002 M) and norbornene (0.75 M) in 0.5 mL of dichloromethane was added solid pentafluoroiodosobenzene (6.0 mg, 0.04 M) in one portion. The mixture was vigorously agitated until homogeneous (ca. 3 min), indicating consumption of the oxidant. The green-brown *N*-alkylhemin solution (λ_{max} at 435 nm) was added to 1.5 mL of dichloromethane on top of an alumina column (2 × 1 cm) in a U-tube precooled to −75 °C ($CO_2(s)$−2-propanol). The solution was loaded onto the column and eluted with 6 mL of diethyl ether/dichloromethane (5:95) to remove the oxidation products and pentafluoroiodobenzene generated in the reaction. The *N*-alkylhemin was then removed from the column with 2 mL of methanol/dichloromethane (25:75). For the duration of the chromatography process, the U-tube and all solvents were kept at or near −70 °C. The fractions were collected from the bottom of the U-tube by disposable pipette until the green hemin eluted with the final solvent mixture. An aliquot was removed from the cold hemin solution and diluted with dichloromethane. A UV−vis spectrum indicates the presence of only the *N*-alkylhemin. The remainder of the hemin solution was warmed to room temperature and allowed to stand for 1−2 h before analysis by gas chromatography, ensuring complete decomposition of the *N*-alkylhemin.

Results

UV−Vis Spectral Change. Previous studies[4,5] have established that *N*-alkylhemins exhibit a Soret band at ca. 435 nm. As was observed with 4,4-dimethyl-1-pentene[4] and norbornene,[5] the same shift of the Soret band from 410 to 435 nm was observed during the epoxidation of allyltrimethylsilane, vinylcyclohexane, styrene, allyl cyanide, allyl chloride, and norbornadiene by TDCPPFeCl−PFIB in the mixed $CH_2Cl_2/CF_3CH_2OH/H_2O$ solvents. The spectral changes showing this observed during the oxidation of allyltrimethylsilane at initial concentrations of 1×10^{-6} M for TDCPPFeCl and 5×10^{-4} M for PFIB

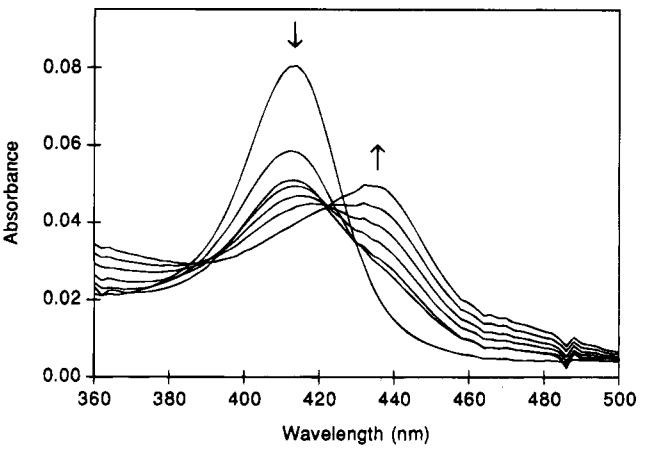

Figure 3. Sequential spectra obtained after mixing to obtain 0.5 M allyltrimethylsilane, 1×10^{-6} M TDCPPFeCl, and 5×10^{-4} M PFIB in 80:18:2 (v/v) $CH_2Cl_2/CF_3CH_2OH/H_2O$. The first spectrum is with the same concentrations of allyltrimethylsilane and TDCPPFeCl, but without PFIB; others are at 6, 9, 12, 18, 30, and 90 s after mixing. Only the Soret region is shown. The small glitches in the spectra at 362, 432, and near 486 nm are due to the HP spectrophotometer.

are shown in Figure 3. Similar spectra changes were observed at higher initial concentrations for PFIB and hemin. The spectral changes are not isosbestic. The spectra observed with styrene, vinylcyclohexane, and allyl chloride showed partial shift of the Soret band and partial return (spectra not shown).[18a]

Quenching Experiments. PFIB reacts rapidly and quantitatively with *trans*-cyclohexane-1,2-diol to form 1,6-hexanedial and pentafluoroiodobenzene.[18b] The bimolecular rate constant measured is approximately 500 M^{-1} s^{-1}. The bimolecular rate constant of the reaction between PFIB and TDCPPFeCl is of the magnitude 10^4 M^{-1} s^{-1}.[19] Therefore, 0.1 M of CHD would efficiently quench the reaction of PFIB (typically $10^{-3}-10^{-5}$ M) with $10^{-6}-10^{-5}$ M of TDCPPFeCl. Final spectra of reactions with allyltrimethylsilane quenched by CHD as a function of time before quenching are presented in Figure 4. The spectra shown are approximately isosbestic. The initial concentrations are the same as those in the experiment shown in Figure 3.

Kinetics. The kinetics of decrease of absorbance at 410 nm and increase of absorbance at 435 nm were measured by stopped-flow spectrophotometry with norbornene, norbornadiene, vinylcyclohexane, styrene, 4,4-dimethyl-1-pentene, and allyltrimethylsilane, using the TDCPPFeCl−PFIB system. The observed rate constants are listed in Table 1.

The kinetics of oxidant disappearance were followed at 280 nm when the initial concentration of PFIB was high, or at 250 nm when the initial concentration of PFIB was low. Although PFIB is quite insoluble in pure dichloromethane, it is soluble enough in the mixed solvents ($CH_2Cl_2/CF_3CH_2OH/H_2O$) to form a solution of known concentration up to 0.01 M. The absorbance changes fit a first-order decrease and afford pseudo-first-order rate constants. The calculated bimolecular rate constants for oxotransfer during the oxidation of 4,4-dimethyl-1-pentene and allyltrimethylsilane by PFIB−TDCPPFeCl in 89:10:1 (v/v) $CH_2Cl_2/CF_3CH_2OH/H_2O$ are $(3 \pm 1) \times 10^4$ M^{-1} s^{-1} and $(4.0 \pm 0.2) \times 10^4$ M^{-1} s^{-1}, respectively. A kinetic trace and the corresponding logarithmic plot at medium turnovers ($[Ox]_0/[Hm]_0 = 50$) are shown in Figure 5. Those obtained at high

(18) (a) Tian, Z.-Q. Ph.D. Dissertation, University of California at San Diego, 1992; pp 29−154. (b) Fann, W.-P. Ph.D. Dissertation, University of California at San Diego, 1992; p 91.

(19) Traylor, T. G.; Marsters, J. C., Jr.; Nakano, T.; Dunlap, B. E. *J. Am. Chem. Soc.* **1985**, *107*, 5537−5539.

Table 1. Rate Constants of Hemin *N*-Alkylation Measured by Stopped-Flow Spectrophotometry[a]

alkenes	$[Ox]_0$	rate constants, 410 nm[c]			rate constants, 435 nm[d]		
		k_{obs}, s^{-1}	$k_{obs}/[Ox]_0$, M^{-1} s^{-1}	return, s^{-1}	k_{obs}, s^{-1}	$k_{obs}/[Ox]_0$, M^{-1} s^{-1}	return, s^{-1}
allyltrimethylsilane	0.002	3.9(0.2)	2000(100)	0.5(0.1)	0.47(0.09)	230(40)	
	0.0005	2.9(0.1)	5800(50)	0.5(0.1)	0.9(0.1)	1800(50)	
	0.0085[b]	6.3(0.2)	740(30)		0.98(0.09)	110(10)	
4,4-dimethyl-1-pentene	0.004	6.4(0.3)	1590(80)		6.2(0.2)	1540(50)	0.48(0.03)
norbornadiene	0.004	4.1(0.6)	1000(200)	0.25(0.04)	4.5(0.2)	1100(50)	0.27(0.03)
norbornene	0.004	1.97(0.05)	500(20)	0.065	2.15(0.05)	540(10)	0.029
styrene	0.004	1.2(0.2)	310(50)				
vinylcyclohexane	0.004	2.0(0.4)	500(90)		4.3(0.4)	1100(100)	0.73(0.03)

[a] Each number listed is the average of several experiments; the standard deviation is given in parentheses. The initial concentration of TDCPPFeCl was 1×10^{-5} M, and the initial concentrations of alkenes are 0.5 M for ATMS, 0.9 M for VCH, and 1 M for others. The solvent used was 89:10:1 (v/v) $CH_2Cl_2/CF_3CH_2OH/H_2O$ unless specified otherwise. [b] The solvent was 80:18:2 (v/v) $CH_2Cl_2/CF_3CH_2OH/H_2O$. [c] Measurements at 410 nm, or 415 nm in some cases. [d] Measurements at 435 nm, or 440 nm in some cases.

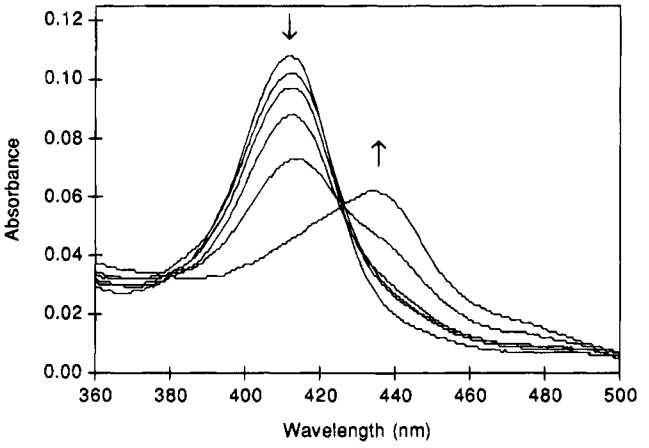

Figure 4. Spectra of solutions obtained from quenching the reaction of FeTDCPPCl (1×10^{-6} M) and allyltrimethylsilane (0.5 M) with PFIB (5×10^{-4} M) in 80:18:2 (v/v) $CH_2Cl_2/CF_3CH_2OH/H_2O$ by adding 1 M CHD solution to achieve 0.1 M of CHD. The quencher was added before PFIB for the first spectrum. Times before quenching are 2, 10, 60, 180, and 600 s for others. Each spectrum was recorded about 20 min after quenching, and only the Soret region is shown. The small steps in the spectra are due to the fact that the digitized output of the Kontron spectrophotometer has a minimum interval of 0.001 absorbance units.

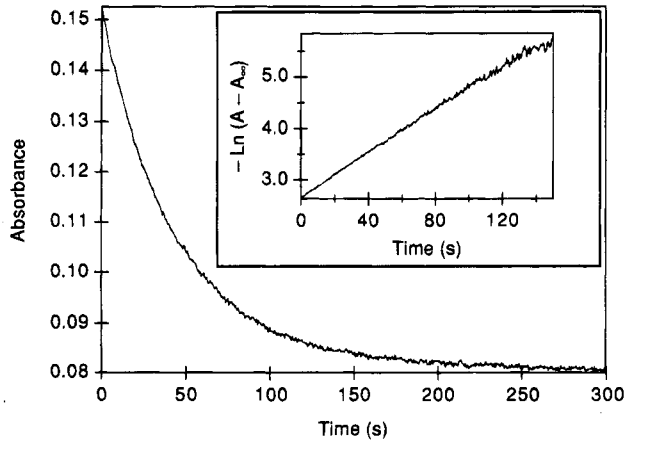

Figure 5. Kinetics of oxidant disappearance at medium turnovers observed at 250 nm. The initial concentrations after mixing were 0.25 M for 4,4-dimethyl-1-pentene, 5×10^{-7} M for TDCPPFeCl, and 2.5×10^{-5} M for PFIB in 89:10:1 (v/v) $CH_2Cl_2/CF_3CH_2OH/H_2O$. Time 0 is approximately 5 s after mixing. About 50% *N*-alkylhemin formation was observed. The ln plot of these data is shown in the inset.

turnovers ($[Ox]_0/[Hm]_0 = 200$) and low turnovers ($[Ox]_0/[Hm]_0 = 10$) are similar.

The hemin-catalyzed oxidation of allyltrimethylsilane and the concomitant *N*-alkylation were also observed by UV−vis spectroscopy under high oxidant concentrations (more than 400 turnovers) in 80:18:2 (v/v) $CH_2Cl_2/CF_3CH_2OH/H_2O$. The rates of *N*-alkylation were calculated using the first half-life of absorbance change at 410 or 436 nm, during which the oxidant disappearance was minimal. A bimolecular rate constant of 260 ± 50 M^{-1} s^{-1} was obtained for experiments with various initial concentrations of the hemin and the oxidant. The kinetics of oxidant disappearance at high turnovers was not first-order. Analysis of the data is presented in the Discussion.

Products of *N*-Alkylhemin Decomposition. As previously reported, TTPFeCl was completely *N*-alkylated during the oxidation of norbornene by PFIB, as indicated by UV−vis spectroscopy.[5,10] The alkylated product is unstable at 25 °C ($t_{1/2} \approx 3$ min),[5,10] but extremely persistent (no decomposition after several hours) at ≤−50 °C. After the reaction mixture was cooled, it was possible to separate the excess reactants and products generated during the oxidation from the *N*-alkyl species formed during this reaction using a short (2 cm) alumina column at low temperatures. After the reaction mixture was rapidly cooled and loaded onto the column, a normal distribution of reactants and products was eluted with diethyl ether/dichloromethane (5:95). The hemin was eluted with methanol/dichloromethane (25:75) and was shown to be the *N*-alkyl species by UV−vis spectroscopy. After several hours at room temperature, the unstable hemin decomposed back to the original catalyst. GC analysis of this solution showed *exo*-2,3-epoxynorbornane to be the only significant norbornene-derived product generated by this decomposition.

Discussion

Transient Formation of Secondary *N*-Alkylhemin by Terminal Alkenes. The formation of primary *N*-alkylhemins during oxidation catalyzed by cytochromes P-450 and model iron porphyrins has been reported previously for many terminal alkenes.[1,4,6] The structures of these *N*-alkylhemins have been well-characterized by NMR, IR, EPR, and mass spectroscopy and elemental analysis. The formation of secondary *N*-alkylhemins with internal alkenes has also been reported.[3c,5,10] Structural evidence for these include UV−vis and EPR spectroscopy. While primary *N*-alkylhemins are stable and can be isolated, the secondary *N*-alkylhemins decompose rapidly and are observed only as transient species. Still, both primary and secondary *N*-alkylhemin species have distinctive UV−vis spectra. All of the *N*-alkylhemins formed during the oxidation of various alkenes by PFIB using TDCPPFeCl as the catalyst have a Soret absorption band at 435 nm.[4,5,10]

When terminal alkenes, including allyltrimethylsilane, vinylcyclohexane, and styrene, are oxidized by TDCPPFeCl and PFIB, they form species with characteristic bands at ap-

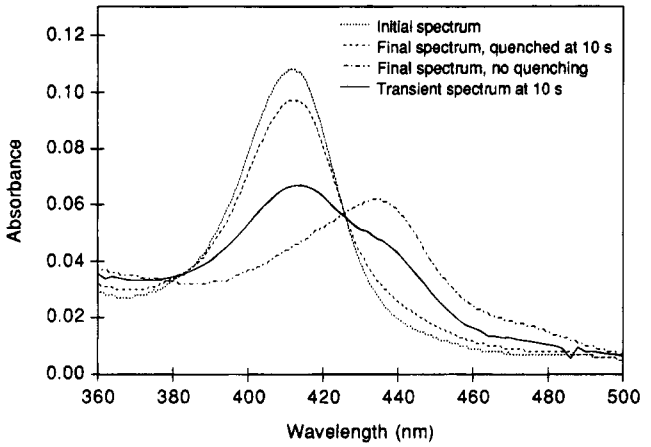

Figure 6. Comparison between quenched and unquenched reactions. Spectra were obtained with 0.5 M allyltrimethylsilane, 1×10^{-6} M TDCPPFeCl, and 5×10^{-4} M PFIB in 80:18:2 (v/v) $CH_2Cl_2/CF_3CH_2OH/H_2O$. The quenching agent was 0.1 M cyclohexane-1,2-diol.

proximately 435 nm. This 435-nm band shifts back to 410 nm over time, but only *partially*, giving a final spectrum that includes a mixture of 410- and 435-nm bands. This suggests that two species are formed, both having absorption bands at 435 nm. One of them is stable and thus persists, while the other one decomposes with time. For a reaction of 0.5 M allyltrimethylsilane, 1×10^{-5} M TDCPPFeCl, and 0.0085 M PFIB in 80:18:2 (v/v) $CH_2Cl_2/CF_3CH_2OH/H_2O$, the transient spectrum at 4 s showed nearly complete *N*-alkylation, while the final spectrum indicated approximately 70% *N*-alkylation. The stable species match what have been described for primary *N*-alkylhemins. Although there is no direct structural proof for the unstable species, by analogy of its UV−vis spectroscopy, the conditions for its formation and decomposition, and its catalytic activity toward epoxidation, the most reasonable assignment for it is the secondary *N*-alkylhemin.

The simultaneous formation of secondary and primary *N*-alkylhemins has also been demonstrated by quenching experiments. It has been established that *N*-alkylation results from the active turnover of alkenes; not from the accumulation of the product epoxide.[1,6,20] Therefore, formation of *N*-alkylhemins requires an oxidant. If the oxidant is quenched at a given time during the reaction, the unstable secondary *N*-alkylhemin reverts back to the original hemin without being realkylated. Any *N*-alkylhemin that remains must be the primary species accumulated until that time. The oxidant used in this study is PFIB. Under typical reaction conditions, 10^{-6}–10^{-5} M TDCPPFeCl is used. As stated earlier, 0.1 M CHD effectively quenches the reaction of PFIB with TDCPPFeCl. A set of final spectra of quenched reactions (Figure 4) appears to be very similar to a set of transient spectra observed during one reaction (Figure 3). However, they have very different time scales. The transient spectra, which show the sum of the primary and the secondary *N*-alkylhemins, show complete conversion in 90 s using 1×10^{-6} M TDCPPFeCl and 5×10^{-4} M PFIB in 80:18:2 (v/v) $CH_2Cl_2/CF_3CH_2OH/H_2O$, whereas complete conversion to the primary *N*-alkylhemin takes up to 600 s. During the excess time, through the turnovers of oxotransfer, the secondary *N*-alkylhemin and the original hemin are approaching a steady state that is dependent on the concentration of the oxidant, while more primary *N*-alkylhemin is accumulated. Figure 6 shows the spectra of the above reaction, in comparison with the spectra of the original hemin and the fully *N*-alkylated hemin.

(20) Ortiz de Montellano, P. R.; Mangold, B. L. K.; Wheeler, C.; Kunze, K. L.; Reich, N. O. *J. Biol. Chem.* **1983**, *258*, 4208–4213.

A similar comparison was observed for the reaction using 1×10^{-5} M TDCPPFeCl and 0.0085 M PFIB. It is obvious that two distinct *N*-alkylhemins form the allyltrimethylsilane. At higher concentrations, the partial reverse is indicated by the comparison of the transient spectrum and the final spectrum; whereas at lower concentrations, the reverse is not obvious on the sequential spectra, because the hemin from the decomposition of the secondary *N*-alkylhemin is immediately converted again to an *N*-alkylhemin. Vinylcyclohexane shows behavior similar to allyltrimethylsilane. Complete *N*-alkylation with styrene and allyl chloride requires even higher concentrations of PFIB. Only partial *N*-alkylation is observed for these substrates using the maximum oxidant concentration possible. Nevertheless, the partial reverse is observed.

Fast Kinetic Measurements. The kinetics for the terminal alkenes are more complicated than the kinetics for norbornene, and the complication is not limited to the fact that norbornene gives one *N*-alkyl species whereas a terminal alkene gives two. The fast kinetics of Soret change at 410 and 435 nm with high concentrations of oxidant and hemin were observed by stopped-flow spectrophotometry. Measurements with norbornene confirm the results of Traylor and co-workers.[5] As shown in Table 1, the initial pseudo-first-order decrease at 410 nm and increase at 435 nm give rates that lead to similar bimolecular rate constants of about 500 M^{-1} s^{-1}, and the reverse change gives a rate constant of 0.6 s^{-1}. Similar rates were obtained at 410 and 435 nm with norbornadiene and 4,4-dimethyl-1-pentane also. With allyltrimethylsilane, an early decrease of absorbance at both 410 and 435 nm (0−0.2 s) was followed by a continuing decrease at 410 nm and increase at 435 nm, which was then followed by a reverse change t 410 nm but continuing increase at 435 nm. This change was also observed on sequential spectra. The initial decrease is possibly due to a hemin axial ligand change upon mixing with PFIB and is not related to *N*-alkylation, because such decrease was also observed by stopped-flow spectrophotometry during the TDCPPFeCl−PFIB oxidation of mesitylene, a process that does not produce *N*-alkylhemin. Because of this initial decrease, the rate measured at 410 nm is several times of that at 435 nm.

The overall increase later in the reaction is probably due to the inhomogeneity that results from accumulation of epoxide and pentafluoroiodobenzene. In order to study the kinetics of iron(III) porphyrin-catalyzed oxidation in a homogeneous system, Traylor and co-workers developed the mixed $CH_2Cl_2/CF_3CH_2OH/H_2O$ (89:10:1 or 80:18:2) solvent system, which can provide reasonable concentrations of PFIB, alkenes, and hemin catalysts.[19] The 1−2% water accelerates the reaction. In the 89:10:1 or the 80:18:2 mixture, the 1% or 2% water, respectively, is the maximum amount of water that can stay in one phase. It seems that in this study of *N*-alkylation, we are reaching the limit of these solvent systems, because the solution turned turbid at the end of the reaction of allyltrimethylsilane (0.5−1 M) using a high concentration of PFIB (0.002 M). The reverse rate (rate of decomposition) is hardly measurable because at low concentration of PFIB, the extent of *N*-alkylation is too small to give an accurate rate; but at high concentration of PFIB, the inhomogeneity interferes. With styrene, the extinction coefficient of the *N*-alkyl species is very small (less than one-third of the hemin), so that the increase of the Soret absorbance of the *N*-alkylhemins at 435 nm cannot compensate for the decrease due to the loss of hemin. Therefore, the rate can be measured only at 410 nm. Despite all the factors discussed above, the approximate rate constants of total *N*-alkylation were estimated ($k_{obs}/[Ox]_0$ in Table 1).

Kinetics of Epoxidation Catalyzed by *N*-Alkylhemins. The

rates of oxotransfer were measured by the absorbance decrease at 250−280 nm, because PFIB has a higher absorbance in this region than pentafluoroiodobenzene. In the 89:10:1 (v/v) $CH_2Cl_2/CF_3CH_2OH/H_2O$ solvent, the kinetics of decrease of oxidant were pseudo-first-order and independent of the concentration of the substrates 4,4-dimethyl-1-pentene and allyltrimethylsilane at either high turnovers or low turnovers. A broad range of PFIB and TDCPPFeCl concentrations were tested, and they led to a final percentage of *N*-alkylhemins ranging from <5% to >90%. Nevertheless, all the experiments showed a pseudo-first-order decrease of absorbance at 250 (or 280) nm, and the bimolecular rate constant calculated was between 2×10^4 and 5×10^4 M^{-1} s^{-1}, which is the same as reported previously.[19] These results suggest that in 89:10:1 (v/v) $CH_2Cl_2/CF_3CH_2OH/H_2O$, the hemin, the primary *N*-alkylhemin, and the secondary *N*-alkylhemin have similar catalytic activities and react with PFIB at similar rates.

In the 80:18:2 (v/v) $CH_2Cl_2/CF_3CH_2OH/H_2O$, however, the kinetics of oxotransfer were not pseudo-first-order. A reaction of 0.5 M allyltrimethylsilane, 5×10^{-7} M TDCPPFeCl, and 1×10^{-4} M PFIB resulted in about 50% *N*-alkylation. The rate constant calculated from the first half-life of the oxidant disappearance is 4.7×10^4 M^{-1} s^{-1}, which corresponds to the catalysis by the hemin because the amount of *N*-alkylation is very limited at the beginning. The second half-life is 1.2 times as long as the first half-life. The catalytic rate constants of the *N*-alkylhemins need to be calculated from the nonexponential absorbance change observed.

The epoxidation of alkenes catalyzed by iron(III) porphyrins is believed to occur via the oxoiron(IV) porphyrin radical cation species.[21−24] Considering the fact that the *N*-alkylhemins are catalysts for epoxidation, the kinetic pathway as shown in Scheme 2 is proposed.

Scheme 2. Kinetic Pathway for Hemin-Catalyzed Epoxidation and *N*-Alkylation

$$\text{Hm} + \text{Ox} \xrightarrow{k_1} \text{HmO} \quad (1)$$

$$\text{HmO} + \text{S} \xrightarrow{k_2} \text{SO} + \text{Hm} \quad (2)$$

$$\text{HmO} + \text{S} \xrightarrow{k_3} 1°\text{-Hs} \quad (3)$$

$$\text{HmO} + \text{S} \xrightarrow{k_4} 2°\text{-Hs} \quad (4)$$

$$2°\text{-Hs} \xrightarrow{k_5} \text{Hm} + \text{organic products} \quad (5)$$

$$1°\text{-Hs} + \text{Ox} \xrightarrow{k_6} 1°\text{-HsO} \quad (6)$$

$$1°\text{-HsO} + \text{S} \xrightarrow{k_7} \text{SO} + 1°\text{-Hs} \quad (7)$$

$$2°\text{-Hs} + \text{Ox} \xrightarrow{k_8} 2°\text{-HsO} \quad (8)$$

$$2°\text{-HsO} + \text{S} \xrightarrow{k_9} \text{SO} + 2°\text{-Hs} \quad (9)$$

where

Hm = hemin or iron(III) porphyrin

HmO = oxoiron(IV) porphyrin radical cation

Hs = *N*-alkylhemin

HsO = oxoiron(IV) *N*-alkylporphyrin radical cation

Ox = oxidant (PFIB)

S = substrate (alkene)

SO = epoxide

We found no evidence for double *N*-alkylation, although it is possible because iron complexes of *N,N'*-bis-alkylporphyrins have been prepared by other methods.[7]

It has been shown that the rate of either oxotransfer or *N*-alkylation is independent of alkene concentration,[6,7,19] and the rate of epoxidation shows little dependence on the structure of the alkene.[25] Formation of the high valent oxoiron species is rate-limiting during alkene epoxidation, and it does not accumulate. It will oxidize another hemin if there is not enough substrate available. Assuming the steady-state approximation for HmO and HsO's, Scheme 2 can be simplified to Scheme 3.

Scheme 3. Simplified Kinetic Pathway

$$\text{Hm} + \text{Ox} + \text{S} \xrightarrow{k_{ox}} \text{SO} + \text{Hm} \quad (10)$$

$$\text{Hm} + \text{Ox} + \text{S} \xrightarrow{k_{na1}} 1°\text{-Hs} \quad (11)$$

$$\text{Hm} + \text{Ox} + \text{S} \xrightarrow{k_{na2}} 2°\text{-Hs} \quad (12)$$

$$2°\text{-Hs} \xrightarrow{k_5} \text{Hm} + \text{organic products} \quad (13)$$

$$1°\text{-Hs} + \text{Ox} + \text{S} \xrightarrow{k_{ox1}} \text{SO} + 1°\text{-Hs} \quad (14)$$

$$2°\text{-Hs} + \text{Ox} + \text{S} \xrightarrow{k_{ox2}} \text{SO} + 2°\text{-Hs} \quad (15)$$

where

$$k_{ox} = \frac{k_1 k_2}{k_2 + k_3 + k_4} \quad (16)$$

$$k_{na1} = \frac{k_1 k_3}{k_2 + k_3 + k_4} \quad (17)$$

$$k_{na2} = \frac{k_1 k_4}{k_2 + k_3 + k_4} \quad (18)$$

$$k_{ox1} = k_6 \quad (19)$$

$$k_{ox2} = k_8 \quad (20)$$

The measured rate constant of total *N*-alkylation ($k_{na} = k_{na1} + k_{na2}$) is about 260 M^{-1} s^{-1} in 80:18:2 (v/v) $CH_2Cl_2/CF_3CH_2OH/H_2O$ for allyltrimethylsilane, and the rate constant of oxidant disappearance measured at low oxidant concentration, when *N*-alkylation is negligible, is about 5×10^4 M^{-1} s^{-1}. The rate of *N*-alkylation is less than 1% of the rate of oxotransfer, i.e., *N*-alkylhemin formation accounts for less than 1% of the oxidant disappearance while epoxide formation accounts for the rest.

(21) Traylor, T. G. *Pure Appl. Chem.* **1991**, *63*, 265−274.
(22) Guengerich, F. P.; Macdonald, T. L. *Acc. Chem. Res.* **1984**, *17*, 9−16.
(23) McMurry, T. J.; Groves, J. T. In *Cytochrome P-450: Structure, Mechanism, and Biochemistry*; Ortiz de Montellano, P. R., Ed.; Plenum: New York, 1986; pp 1−28.
(24) Okamoto, T.; Sasaki, K.; Tachibana, M. *Bull. Inst. Chem. Res., Kyoto Univ.* **1989**, *67*, 169−195.
(25) Traylor, T. G.; Xu, F. *J. Am. Chem. Soc.* **1988**, *110*, 1953−1958.

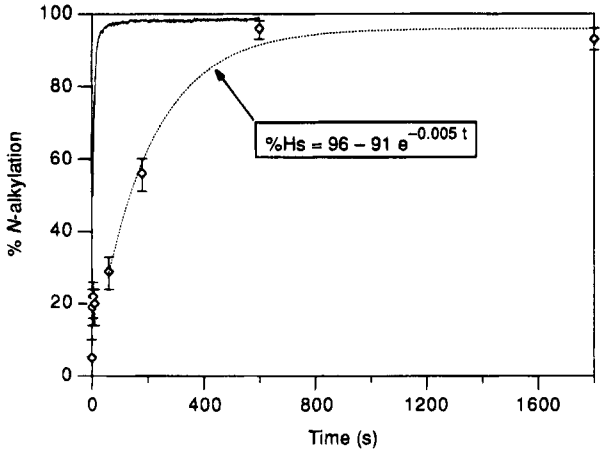

Figure 7. Comparison between total *N*-alkylation and primary *N*-alkylation as a function of time. The solid line at the upper-left corner is the absorbance change at 436 nm for a solution of 0.5 M allyltrimethylsilane, 1×10^{-6} M TDCPPFeCl, and 5×10^{-4} M PFIB in 80:18:2 (v/v) $CH_2Cl_2/CF_3CH_2OH/H_2O$. The first point is 5 s after mixing. The data points shown as diamonds are calculated percent *N*-alkylation from the quenching experiments shown in Figure 6. The dotted line is the exponential fit for the last four data points.

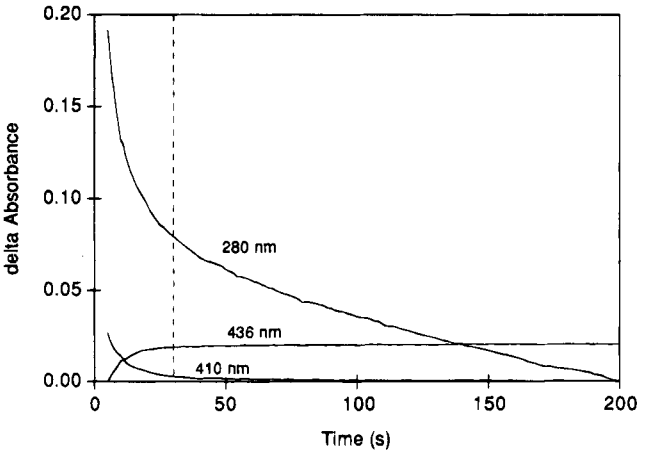

Figure 8. Kinetics of absorbance change at 280, 410, and 436 nm for a solution obtained by mixing a solution of allyltrimethylsilane (1 M) and TDCPPFeCl (1×10^{-6} M) in 80:18:2 (v/v) $CH_2Cl_2/CF_3CH_2OH/H_2O$ with equal volume of PFIB (2×10^{-4} M) in the same solvent.

Therefore, $k_{ox} \approx k_1 \gg k_{na}$ or $k_2 \gg (k_3 + k_4)$. The rate of oxidant disappearance approximately equals the rate of epoxide formation.

In the 80:18:2 solvent with allyltrimethylsilane, k_{ox}, k_{ox1}, and k_{ox2} are different, so the observed oxidant disappearance is not pseudo-first-order. At high turnovers and reasonable oxidant concentrations (e.g. $[Hm]_0 = 1 \times 10^{-6}$ M, $[Ox]_0 = 5 \times 10^{-4}$ M, 500 turnovers), the hemin is alkylated quickly and completely to form a mixture of the primary and secondary *N*-alkylhemins. The reverse rate of the secondary *N*-alkylhemin is slow (the estimated value is $0.01-0.02$ s^{-1} as shown later in this discussion) compared to the rate of formation ($k_{na}[Ox] \approx 0.13$ s^{-1}). So the composition of the *N*-alkylhemin mixture is determined by the rates of formation, i.e., $[2°\text{-Hs}]/[1°\text{-Hs}] = k_{na2}/k_{na1}$. As observed in the experiments shown in Figures 3 and 4, the total *N*-alkylation is nearly 100% in less than 90 s of reaction. At this time, the concentration of the secondary *N*-alkylhemin reaches its maximum, which can be calculated according to eq 21.

$$[2°\text{-Hs}]_{max} = \frac{k_{na2}}{k_{na1} + k_{na2}}[Hm]_0 \tag{21}$$

After [2°-Hs] reaches its maximum, the seconary *N*-alkylhemin transforms into the primary *N*-alkylhemin through the hemin in the presence of the oxidant (eq 22), and the primary species is accumulated. All three species catalyzed epoxidation. Figure 7 shows the comparison between total *N*-alkylation (indicated by the absorbance change at 436 nm) and primary *N*-alkylation (determined from the quenching experiments shown in Figure 4) as a function of time observed with the reaction of allyltrimethylsilane in 80:18:2 (v/v) $CH_2Cl_2/CF_3CH_2OH/H_2O$ with 1×10^{-6} M TDCPPFeCl and 5×10^{-4} M PFIB. *N*-Alkylation is near completion in a very short time, but the accumulation of the primary *N*-alkylhemin is much slower.

$$2°\text{-Hs} \underset{k_{na2}[Ox]}{\overset{k_5}{\rightleftharpoons}} Hm \xrightarrow{k_{na1}[Ox]} 1°\text{-Hs} \tag{22}$$

At a high oxidant concentration, i.e., $k_{na2}[Ox] > k_5$, the decomposition of the secondary *N*-alkylhemin is the rate-limiting step. As shown in Figure 7, the hemins stay *N*-alkylated during the transformation. Thus with steady-state approximation for [Hm] the kinetics for eq 22 can be solved.

$$-\frac{d[2°\text{-Hs}]}{dt} = \frac{k_5 k_{na1}}{k_{na1} + k_{na2}}[2°\text{-Hs}] \tag{23}$$

$$\ln \frac{[2°\text{-Hs}]_{max}}{[2°\text{-Hs}]} = \frac{k_5 k_{na1}}{k_{na1} + k_{na2}} t \tag{24}$$

or

$$[2°\text{-Hs}] = [2°\text{-Hs}]_{max} e^{-k_c t} \tag{25}$$

where

$$k_c = \frac{k_5 k_{na1}}{k_{na1} + k_{na2}} \tag{26}$$

Note that in eqs 24 and 25, the time t is set to zero at the point when [2°-Hs] maximizes. Exponential fit of the primary *N*-alkylhemin formation from the secondary *N*-alkylhemin gives an estimate of the rate constant of conversion (k_c), which is about 0.005 s^{-1}. The values for k_{na1} and k_{na2} can be estimated from Figure 6. At 10 s, the reaction is in the phase of simultaneous primary and secondary *N*-alkylation. The transient spectrum shows about 60% total *N*-alkylation, and the spectrum after quenching at 10 s shows about 15% of primary *N*-alkylation. Thus $k_{na1}/(k_{na1} + k_{na2}) = 0.25$, or $k_{na2}/k_{na1} = 3$. With the total $k_{na} = 260$, the estimated values are $k_{na1} = 60$ and $k_{na2} = 200$. We obtain $k_5 = 0.02$ s^{-1}.

The absorbance change at 280, 410, and 436 nm for a reaction with high turnovers is shown in Figure 8. The dotted line markes the approximate time when the [2°-Hs] reaches its maximum. After this point, the main catalysts for epoxidation are the *N*-alkylhemins, so reactions shown in eqs 14 and 15 contribute to most of the oxidant disappearance (eq 27). With

$$-\frac{d[Ox]}{dt} = k_{ox1}[1°\text{-Hs}][Ox] + k_{ox2}[2°\text{-Hs}][Ox] \tag{27}$$

eqs 21 and 25,

$$[1°\text{-Hs}] = [Hm]_0 - [2°\text{-Hs}] = \left(1 - \frac{k_{na2}}{k_{na1} + k_{na2}} e^{-k_c t}\right)[Hm]_0 \tag{28}$$

$$-\frac{d[Ox]}{[Ox]} = \left\{k_{ox1} + \frac{(k_{ox2} - k_{ox1})k_{na2}}{k_{na1} + k_{na2}} e^{-k_c t}\right\}[Hm]_0\, dt \quad (29)$$

$$-\ln\frac{[Ox]}{[Ox]_0} = \left\{k_{ox1}t + \frac{(k_{ox2} - k_{ox1})k_{na2}}{k_5 k_{na1}}(1 - e^{-k_c t})\right\}[Hm]_0 \quad (30)$$

The oxidant concentration is monitored by absorbance change at 280 nm. Combining eqs 30 and 31, an absorbance−time

$$\frac{[Ox]}{[Ox]_0} = \frac{(A - A_\infty)}{(A_0 - A_\infty)} \quad (31)$$

relationship is established as in eq 32.

$$A = c_0 + c_1 e^{-c_2 t} e^{-c_3(1-e^{-c_4 t})} \quad (32)$$

where

$$c_0 = A_\infty$$

$$c_1 = A_0 - A_\infty$$

$$c_2 = k_{ox1}[Hm]_0$$

$$c_3 = \frac{(k_{ox2} - k_{ox1})k_{na2}}{k_5 k_{na1}}[Hm]_0$$

$$c_4 = k_c = \frac{k_5 k_{na1}}{k_{na1} + k_{na2}}$$

The kinetics of oxidant disappearance were observed with allyltrimethylsilane in 80:18:2 (v/v) $CH_2Cl_2/CF_3CH_2OH/H_2O$ at several concentrations of hemin ($[Hm]_0 = 5 \times 10^{-7}$ to 1.5×10^{-6} M) and oxidant ($[Ox]_0 = 2.5 \times 10^{-4}$ to 7.5×10^{-4} M), keeping the turnover number around 500. The absorbance change at 280 nm was fitted to eq 32. The initial values for c_0 and c_1 are taken from the kinetic trace. A simple double-exponential fit to the curve provides estimates for k_{ox2} and k_{ox1}, which are used with the estimates for k_5 and k_{na2}/k_{na1} to calculate initial values for c_2, c_3 and, c_4. The fit gives reproducible values for c_0, c_1, and c_2, despite quite different initial values. Both c_3 and c_4 have greater uncertainty, but their product (eq 33) is reproducible with different initial values.

$$c_3 c_4 = \frac{(k_{ox2} - k_{ox1})k_{na2}}{k_{na1} + k_{na2}}[Hm]_0 \quad (33)$$

With this fit and the ratio k_{na2}/k_{na1}, k_{ox1} and k_{ox2} were obtained. The average values are $(5 \pm 1) \times 10^3$ M^{-1} s^{-1} for k_{ox1} and $(8 \pm 3) \times 10^4$ M^{-1} s^{-1} for k_{ox2}. An example of the fit is shown in Figure 9. Because of the uncertainty in c_3 and c_4, the decomposition rate constant of the secondary *N*-alkylhemin cannot be obtained from this fit. All the rate constants in Scheme 3 are obtained for allyltrimethylsilane in 80:18:2 (v/v) $CH_2Cl_2/CF_3CH_2OH/H_2O$ and are summarized in Table 2.

Partition Ratios. A partition ratio is the number of oxotransfer turnovers of the catalyst per *N*-alkylation event. A higher partition ratio means a low efficiency of inactivation in the case of cytochrome P-450 or a low rate of *N*-alkylation relative to the rate of oxotransfer in the case of our model iron(III) porphyrins, because the *N*-alkylhemins formed are also catalysts for the alkene oxidation.

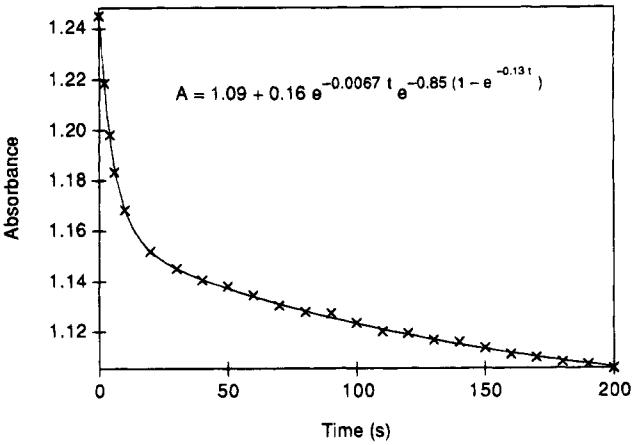

Figure 9. Kinetics of oxidant disappearance observed at 280 nm after mixing a solution of allyltrimethylsilane (1 M) and TDCPPFeCl (3×10^{-6} M) in 80:18:2 (v/v) $CH_2Cl_2/CF_3CH_2OH/H_2O$ with an equal volume of PFIB (1.5×10^{-3} M) in the same solvent. The line is calculated from fitting the experimental data to eq 32. The equation of the line is shown in the figure. The experimental data is marked at every 10th point for the first 30 points and at every 50th point for the rest. Time 0 is about 10 s after mixing.

Table 2. Rate Constants for Allyltrimethylsilane in 80:18:2 (v/v) $CH_2Cl_2/CF_3CH_2OH/H_2O$

rate constants	values	rate constants	values
k_{ox}	5×10^4 M^{-1} s^{-1}	k_{na1}	60 M^{-1} s^{-1}
k_{ox1}	5×10^3 M^{-1} s^{-1}	k_{na2}	200 M^{-1} s^{-1}
k_{ox2}	8×10^4 M^{-1} s^{-1}	k_5	0.02 s^{-1}

Ostovic and Bruice[26] measured partition ratios by determining the amount of epoxide product when the *N*-alkylation was judged as complete from unquenched reaction aliquots. This method neglects the catalytic activity of the *N*-alkylhemins. Collman and co-workers[6] measured the partition ratios by computer-fitting the epoxidation vs time to a reaction scheme that considers the catalytic activity of the primary *N*-alkylhemin, which is the only *N*-alkylhemin observed by their method. Both groups used a heterogeneous reaction system, and the epoxides and *N*-alkylhemins were analyzed from the final product of reaction aliquots.

Formation of the unstable secondary *N*-alkylhemin has to be studied by the kinetic method in a homogeneous system. The partition ratios measured from product analysis become invalid because of the reversible formation of the secondary *N*-alkylhemin and its ability to catalyze epoxidation. In our studies, the partition ratios are measured by the ratio of the rate of oxotransfer to the rate of *N*-alkylation.

$$\text{partition ratio} = \frac{k_{ox}}{k_{na}} = \frac{k_{ox}}{k_{na1} + k_{na2}} = \frac{k_2}{k_3 + k_4} \quad (34)$$

The partition ratio measured for allyltrimethylsilane with TDCPPFeCl in 80:18:2 (v/v) $CH_2Cl_2/CF_3CH_2OH/H_2O$ is about 100. The partition ratios measured for several alkenes with TDCPPFeCl in 89:10:1 (v/v) $CH_2Cl_2/CF_3CH_2OH/H_2O$ are listed in Table 3. The rate constant of around 3×10^4 M^{-1} s^{-1} for oxotransfer is independent of the alkene structures. These alkenes have quite different relative reactivities toward formation of epoxides under competitive conditions. From measurements using the competition methods,[21,25] norbornene is about 30 times as reactive as vinylcyclohexane toward epoxidation, but they

(26) Ostovic, D.; Bruice, T. C. *J. Am. Chem. Soc.* **1989**, *111*, 6511−6517.

Table 3. Partition Ratios Measured by Kinetic Method[a]

alkenes	partition ratios	alkenes	partition ratios
allyltrimethylsilane	100	norbornene	60
4,4-dimethyl-1-pentene	20	styrene	100
norbornadiene	30	vinylcyclohexane	60

[a] The numbers are for the TDCPPFeCl–PFIB system in 89:10:1 (v/v) $CH_2Cl_2/CF_3CH_2OH/H_2O$.

have approximately the same partition ratios. This may suggest that the *N*-alkylation and epoxidation have similar pathways.

Product Analysis of *N*-Alkylhemin Decomposition. The secondary *N*-alkylhemins decompose under reaction conditions at room temperature while the primary *N*-alkylhemins decompose only at higher temperatures.[10] Because epoxidation is always the predominant reaction and an excess of alkene needs to be used to protect the hemin from oxidative destruction, the product analysis of *N*-alkylhemin decomposition requires separation of the *N*-alkylhemin from the products of epoxidation. Studies of the decomposition product of the isolated primary *N*-alkylhemin from 4,4-dimethyl-1-pentene and TDCPPFeCl were inconclusive.

In order to better understand the relationship between epoxidation and alkylation, we have determined the decomposition products of the *N*-alkylhemin from norbornene and TTP-FeCl. The *N*-alkylhemin was isolated and allowed to decompose at room temperature. Analysis by GC indicates that the decomposition affords *exo*-2,3-epoxynorbornane as the major, if not only, product derived from norbornene. It is clear from this observation that decomposition of the *N*-alkylhemin is not responsible for the production of rearranged oxidation products observed in the oxidation of norbornene by this model system.[27,28] Apparently the *N*-alkylhemin generated by an *endo*-attack on norbornene is either too hindered to form at all or too unstable to accumulate during the course of the oxidation reaction. This observation also suggests that the decomposition of other *N*-alkylhemins will also afford epoxide. Given the concept of microscopic reversibility and the fact that both the oxidation reaction and reversal of *N*-alkylation give epoxides as the major products, it seems likely that the two reactions are intimately related.

(27) Traylor, T. G.; Nakano, T.; Dunlap, B. E.; Traylor, P. S.; Dolphin, D. *J. Am. Chem. Soc.* **1986**, *108*, 2782–2784.
(28) Traylor, T. G.; Miksztal, A. R. *J. Am. Chem. Soc.* **1989**, *111*, 7443–7448.

Conclusions

The *N*-alkylhemin formation concomitant with iron(III) porphyrin-catalyzed epoxidation of alkenes was studied in a homogeneous system using PFIB as the oxidant. A second *N*-alkyl species other than the well-documented primary *N*-alkylhemin is observed during the oxidation of terminal alkenes. It is unstable and decomposes under the reaction conditions. Like the primary *N*-alkylhemin, it is a catalyst for alkene epoxidation by PFIB. The characteristics of this transient species are consistent with the secondary *N*-alkylhemin.

Since the iron(III) porphyrin system using PFIB as the oxygen donor has mimicked cytochromes P-450 so well, it probably does not fail in this case. Terminal and internal alkenes may also form the secondary *N*-alkylated species with cytochromes P-450. But because of their instability, they do not result in the "green pigment". However, the formation of the secondary *N*-alkyl species in cytochrome P-450 does inhibit its catalytic activity, because the iron protoporphyrin IX has only one face available for oxidation. The behavior would resemble the reversible inhibition of cytochrome P-450 by ligand binding to the iron center.

The partition ratios have been estimated by a kinetic method in a homogeneous system. This method provides information about the true kinetic partitioning of epoxidation and *N*-alkylation, which can help in elucidating the mechanism of both processes.

Acknowledgment. We thank Professor Charles L. Perrin for his useful comments and his supervision since the death of Professor Teddy G. Traylor and Brenda Leake for her assistance in preparing the manuscript. We are grateful to the National Science Foundation (Grant CHE 87-21364) and the National Institutes of Health (Grant HL13581) for support of this research.

JA932499L